Water retention and pore size distribution in organic soils from tropical mountain peatlands under forest and grassland

Diego Tassinari[1], Pablo G.S. Soares[2], Camila R. Costa[1],
Uidemar M. Barral[3], Ingrid Horák-Terra[4], Alexandre C. Silva[5], William J. Carmo[1]

[1] Postgraduate Program, Federal University of the Jequitinhonha and Mucuri Valleys, Diamantina MG, Brazil
[2] Agronomist, Ipatinga MG, Brazil
[3] Institute of Geociences, University of Brasilia, Brasilia DF, Brazil
[4] Institute of Agrarian Sciences, Federal University of the Jequitinhonha and Mucuri Valleys, Unaí MG, Brazil
[5] Department of Forestry, Federal University of the Jequitinhonha and Mucuri Valleys, Diamantina MG, Brazil

SUMMARY

Peatland soils can store large amounts of water and their retention capacity depends upon soil structure, vegetation type and degree of decomposition. In the Serra do Espinhaço Meridional (south-eastern Brazil), numerous peatlands occur in the headwaters of several watercourses that feed rivers of uttermost importance. The present study aimed to characterise the water retention curves for two peatlands under forest and grassland vegetation. Four peat cores were collected, then sampled every 15 cm. Undisturbed samples were used for water retention analysis and disturbed samples for organic matter characterisation. Water retention data fitted well to bimodal sigmoid retention curves, indicating that the porous system is composed of at least two subsystems with different retention behaviours. One subsystem follows a smooth sigmoid trend at higher matric potentials, while the other subsystem accounts for the steep decrease in water content beyond matric potentials around -7,000 cm. The pore size distribution also reflected this bimodal behaviour, with two distinct peaks around 50 and 0.4 µm. Water retention was predominantly affected by bulk density, which reflected the differences in mineral and organic matter content. The degree of decomposition and lignocellulosic composition of the organic matter also significantly affected water retention, especially at lower matric potentials.

KEY WORDS: bimodal water retention curve, Brazil, Espinhaço Range, Histosol, van Genuchten model

INTRODUCTION

Peatlands are ecosystems originating from the accumulation of organic matter wherever the decay of plant residues is restricted, most often by waterlogging (Takada *et al.* 2016). Their enormous ecological importance stems from their ability to store large amounts of water and organic carbon (Bispo *et al.* 2016, Leng *et al.* 2019). Peatlands are responsible for as much as one fifth to one third of the global soil carbon pool (Yu *et al.* 2010, Treat *et al.* 2019). In addition to storing water, peatlands regulate the flow of watercourses, as they slowly release the water stored during rainy seasons throughout the drier periods of the year (Bispo *et al.* 2016). Because organic residues accumulate through time, peatlands also store several elements that can be used as proxies for assessing past climate and ecological conditions, such as stable isotopes (Horák-Terra *et al.* 2014, 2015; Kock *et al.* 2019), plant phytoliths and pollen (Horák-Terra *et al.* 2020, Kelly *et al.* 2020), and preserved organisms (van Bellen *et al.* 2016).

The great importance of peatlands as water reservoirs can be attributed to two major factors. As wetlands, peatlands occur in depressions within the landscape that receive surface and subsurface water fluxes from upslope (Finlayson & Milton 2018, Lindsay 2018). In addition to receiving much of the water flowing in the landscape, the organic materials that form peatlands can hold as much water as 17 times their own weight (Campos *et al.* 2011). This "sponge-like" behaviour (Silva *et al.* 2013a) is particularly important under climates with strong seasonality in rainfall distribution since it allows peatlands to store water during the rainy season and release it during dry periods.

Water retention in peatlands is affected by the origin and degree of decomposition of the organic residues (Gnatowski *et al.* 2010, Kurnain 2019, Liu & Lennartz 2019), which exhibit distinct differences in behaviour between the less decomposed and more porous acrotelm (surface layers) and the more

decomposed and less porous layers of the deeper catotelm (Dimitrov & Lafleur 2021). The aboveground vegetation also influences the hydraulic behaviour of peatland soils, with differences in water retention depending on the predominance of moss, grassland, or woody vegetation (Kurnain 2019, Liu & Lennartz 2019).

Assessing water retention in peatland Histosols is important for accurate hydrological modelling in these ecosystems (Dimitrov & Lafleur 2021, Taufik *et al.* 2019). Water retention characteristics strongly affect the specific yield (change in water table depth resulting from precipitation) on peatlands with slightly deeper water tables, e.g. below 15 cm (Dettmann & Bechtold 2016). Because of the shallow water table, hydraulic equilibrium can be assumed and thus the water table depth can be used to estimate water content if the water retention characteristics of the soil are known (Dimitrov & Lafleur 2021). The sigmoid water retention curve from van Genuchten (1980) is often applied to peat retention data (e.g. Liu & Lennartz 2019, Dimitrov & Lafleur 2021), but multimodal models have also been used, frequently yielding better results due to the bimodal (Dettmann *et al.* 2014) or even trimodal (Weber *et al.* 2017) pore size distribution of peat. Other challenges for assessing water retention in peatland soils include shrinking and increased hydrophobicity upon drying (Bechtold *et al.* 2018), and extremely high porosity, which make collecting undisturbed samples particularly difficult (Weber *et al.* 2017).

The highlands of the Serra do Espinhaço Meridional in south-eastern Brazil harbour numerous peatlands, owing to the combined effects of resilient organic matter, waterlogging and lower temperatures associated with high altitude (Silva *et al.* 2019, 2020). These peatlands cover more than 142 km^2 (1.2 % of the Serra do Espinhaço Meridional) and store, in an average depth of 1.19 m, 428 Mg ha^{-1} of carbon and almost 1,000 mm (994.8 L m^{-2}) of water (Silva *et al.* 2013a). Although several studies have been conducted to assess their potential as carbon (C) and water reservoirs (Campos *et al.* 2011, 2012; Silva *et al.* 2013a, Bispo *et al.* 2016), these peatlands have not yet been properly characterised in terms of their water retention characteristics.

We hypothesised that water retention and pore size distribution in mountain peatland soils is affected by soil structure and organic matter composition. The objectives of the present study were to assess the total water holding capacity and the water retention characteristics of tropical mountain peatlands under forest and grassland vegetation, and to investigate the influence of organic matter composition upon water retention.

METHODS

Study sites and sampling

The sampled peatlands are located in the Serra do Espinhaço Meridional, a proterozoic orogenic belt that stretches longitudinally across Minas Gerais and Bahia states in eastern Brazil (Figure 1). The Espinhaço Range is composed mostly of quartzites and phyllites, from which shallow, sandy and poor soils develop, mostly Entisols and Inceptisols (Silva 2005). In several depressions and headwaters, the prevailing hydromorphic conditions favour the accumulation of organic deposits, initiating the formation of peatlands (Horák-Terra *et al.* 2014, Campos *et al.* 2017). These peatlands store large amounts of water, releasing it throughout the year to the countless watercourses that originate there (Bispo *et al.* 2016).

Two peatlands were selected for the present study, one located in the Pinheiro district (called Pinheiro peatland) at 1,220 m a.s.l., and the other in the São João da Chapada district (called Chapada peatland) at 1,330 m a.s.l., both in the municipality of Diamantina in Minas Gerais state (Figure 1). Average annual temperature is 18.7 °C, with average minimum temperature 11.3 °C in July and average maximum temperature 26 °C in February (INMET 2022). Average annual rainfall is 1,375 mm, 89 % of which is concentrated during the rainy season which lasts from October to March (INMET 2022).

At each peatland, two cores were collected, one under grassland vegetation and the other under forest vegetation. Grassland (*campo úmido*) is the main vegetation type in these peatlands, but forest fragments occur as patches (called *capões*) dispersed throughout the peatlands (Figure 2). The *campo úmido* vegetation is dominated not only by grasses (Poaceae) but also by species from the families Cyperaceae, Xyridaceae and Eriocaulaceae which are typical of these waterlogged environments (Silva *et al.* 2013b, Silva *et al.* 2019). The *capões* are composed of a mixture of Atlantic rainforest species, mainly from the semideciduous seasonal forest and the montane forest phytophysiognomies. These *capões* are thought to be remnants of more extensive forests that developed under colder and wetter climates in the Quaternary Period (Silva *et al.* 2019, Horák-Terra *et al.* 2020).

The peat cores were collected in 3.0 m long aluminium tubes of 76 mm external diameter (wall thickness 3.2 mm). These tubes were inserted vertically into the peatlands with vibration provided by a stationary engine, causing minimum disturbance to the sampled material (Martin *et al.* 1995). When the basal layer of the peat deposit was reached (90–

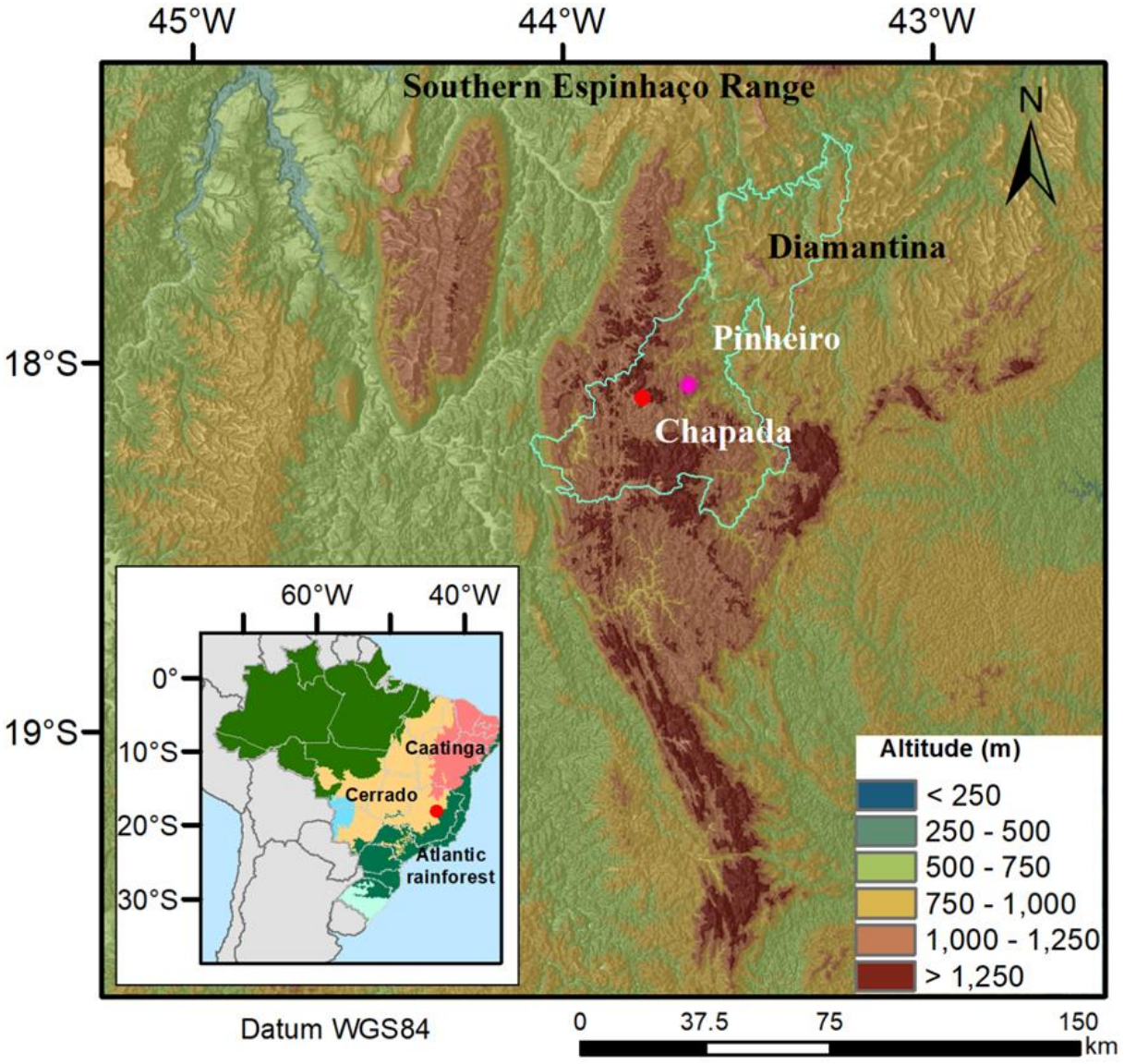

Figure 1. Locations of the studied peatlands (Pinheiro and Chapada) in the Serra do Espinhaço Meridional, Minas Gerais (MG) state, south-eastern Brazil.

135 cm depending on the site), the vibration ceased and a sealing cap was placed on the upper end of the tube. The core was then hoisted using a tripod-mounted pulley and the lower end was also covered with a cap (Figure 2). The core was transported in a semi-vertical position to prevent mixing of different layers.

Laboratory analysis

In the laboratory the aluminium tubes were cut longitudinally with an electric saw to expose the peat cores. Undisturbed samples for evaluation of the water retention curve were collected from the cores at 15 cm depth intervals using PVC rings (4.8 cm height and 4.7 cm internal diameter on average), that were carefully inserted into the exposed face of the core. Samples were collected only from the organic layers, as indicated by the morphological description of the core, meaning that sampling continued to different depths in different cores depending on the thickness of the organic layer. During this process, disturbed samples were also collected for chemical characterisation of the peat layers. Analytical procedures followed Brazilian standards (Teixeira *et al.* 2017).

A nylon cloth was attached to the bottom of the ring containing each undisturbed sample to prevent loss of material. The samples were then placed in plastic trays and saturated by slowly filling the trays with distilled water. After saturation, the samples were weighed and equilibrated at a range of water tensions (100, 1000, 3,000, 7,000 and 15,000 cm) in

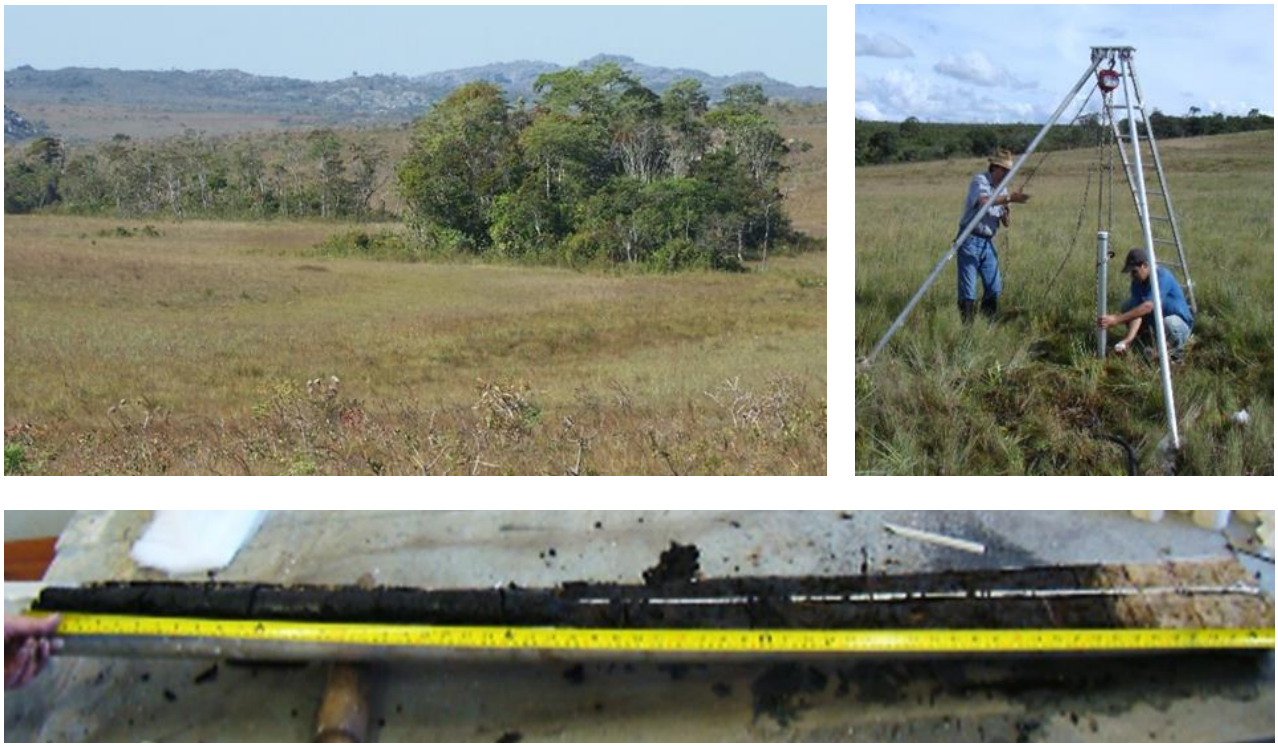

Figure 2. Top left: Peatland vegetation in the Serra do Espinhaço is dominated by grassland (*campo úmido*) with patches of forest vegetation (*capões*). Top right: Peat core being hoisted using a pulley mounted on a tripod. Bottom: Peat core exposed after cutting the aluminium tube open (notice the yellowish mineral basal layer at the bottom).

porous plate extractors (Teixeira & Bhering 2017). Following each step, the samples were weighed to determine water content (θ, $m^3\ m^{-3}$). After the final step, the samples were oven-dried (50 °C for 48 h) and weighed to enable calculation of the soil bulk density (ρ, $Mg\ m^{-3}$).

The disturbed samples were dried (50 °C for 12 h) and sieved (2 mm) prior to analysis. Organic and mineral matter content were determined by combustion of the samples in a muffle furnace at 500 °C for 3 h (Fontana 2017). Mineral matter content was considered equal to the residue following combustion, whereas the organic matter content was considered equal to the amount of material lost (loss on ignition). The organic and mineral matter contents were multiplied by the bulk density values of the respective layers to express the soil composition in terms of specific weight (mass of organic material per unit volume of peat).

Weight distribution of humic substances was determined by the standard alkali-acid extraction procedure (Benites *et al.* 2017). Initially, the fulvic and humic acids fraction was extracted with NaOH (0.1 mol L^{-1}). Following centrifugation, the supernatant (fulvic acids + humic acids fraction) was acidified (HCl; 6 mol L^{-1}) and centrifuged, thus separating the fulvic acids fraction (supernatant) from the humic acids fraction (precipitate). The soluble fractions were oven dried (45 °C) and weighed. The precipitate from the alkali extraction contained the soil minerals and the humin fraction. This precipitate was calcinated at 600 °C for 4 h and the weight loss was considered equal to the weight of the humin fraction.

Rubbed and unrubbed fibre contents were determined according to Lynn *et al.* (1974). The moist organic material was packed into a 5 mL syringe cut in half longitudinally (volume 2.5 mL) then washed with water into a 0.149 mm (100 mesh) sieve. The retained material was repacked into the half-syringe and its volume, corresponding to the fraction of unrubbed fibre, was measured. This material was washed again in the sieve whilst being gently rubbed between the fingers. The remaining material was again packed into the half syringe and its volume corresponded to the fraction of rubbed fibre.

Organic elemental composition (C and N content) was determined by combustion in an elemental analyser (LECO TruSpec) according to Fontana & Bianchi (2017). The C and N contents were expressed as proportions of total organic matter

content (proportion of C and N in the organic matter) to better represent degree of decomposition. The C and N contents were also expressed in relation to each other as a quotient (C:N ratio).

For isotope determination, the dried samples were crushed in an agate mortar and weighed in metallic capsules. The content of ^{13}C was determined in a mass spectrometer and expressed as $\delta^{13}C$ (isotopic abundance of ^{13}C in relation to ^{12}C). More negative $\delta^{13}C$ values are linked to a predominance of C_3 plants (trees and herbaceous plants of wet environments), while less negative $\delta^{13}C$ values are linked to a predominance of C_4 plants (grasses from open and drier environments).

Lignocellulosic composition of the organic material was determined according to the method proposed by van Soest (1994) for bromatological analysis of forage materials. The lignin and cellulose were extracted with an acid detergent that solubilises other cellular components. Cellulose content was determined after oxidation of lignin with acetic acid and potassium permanganate. Lignin content was determined following oxidation of cellulose with sulfuric acid. The lignin and cellulose contents were determined following digestion by combustion of the residues in a muffle furnace (500 °C for 3 h).

Statistical analysis

Water retention data were fitted to bimodal van Genuchten water retention curves (van Genuchten 1980, Durner 1994).

$$\theta = \theta_r + (\theta_s - \theta_r) \sum_{i=1}^{k} w_i \frac{1}{[1+ (\alpha_i|h|)^{n_i}]^{m_i}} \quad [1]$$

where:

- θ is the volumetric water content ($m^3\ m^{-3}$);
- θ_r is the residual water content ($m^3\ m^{-3}$), defined as the water content at water potential -15,000 cm;
- θ_s is the water content at saturation ($m^3\ m^{-3}$);
- k is the number of subsystems in the multi-modal water retention curve - given the restricted number of observations (six ordered pairs of θ, h), k was fixed at 2, making the water retention curves bimodal (composed of two subsystems);
- w_i is the relative weight of each of the k subsystems (an adjusted parameter of the fitting procedure) - since the water retention was bimodal and the sum of w_i values was unity, only w_1 was fitted and w_2 was calculated as $w_2 = 1 - w_1$;
- $|h|$ is the modulus of matric potential (pressure head) (cm);
- α_i and n_i are adjusted parameters for each of the subsystems; and
- m_i is also an adjusted parameter, but we adopted $m = 1 - (1/n)$ following Mualem (1976).

The fitting procedure was performed with the Solver tool in Microsoft Excel, by minimising the sum of squared errors. The target value (sum of squared errors) was minimised by changing the values of the adjusted parameters. The parameters θ_r and θ_s were not fitted and their observed values were used, as only five adjusted parameters (w_1, α_1, α_2, n_1, n_2) were allowed (given that there were six observations per curve). The quality of the fitted equations was assessed in terms of root of mean-squared error (RMSE) and R^2 (square of the correlation coefficient between observed and fitted values).

The pore size distribution was expressed as discrete pore size classes and as a continuous distribution. The classification of pore sizes was modified from de Jong van Lier (2020) and included macropores (equivalent pore diameter > 30 µm), mesopores (equivalent pore diameter 3–30 µm), micropores (equivalent pore diameter 0.2–3 µm) and cryptopores (equivalent pore diameter < 0.2 µm). Although arbitrary, these size classes are related to different pore functions (aeration and water infiltration, retention of readily available water, retention of less available water, and retention of unavailable water, respectively). The continuous pore size distribution was obtained from the first derivative of the water retention curve.

The matric potential values were transformed to equivalent pore diameters using the capillarity equation that, in a simplified form, can be expressed as:

$$\varnothing_{eq} = \frac{2976}{|h|} \quad [2]$$

where $\varnothing_{eq}$ is the equivalent pore diameter (equivalent to the diameter of a capillary) in µm, h is the water potential in cm, and 2976 comprises the constants (contact angle = 0°, surface tension = 0.073 N m^{-1}, specific weight = 1,000 kg m^{-3} and acceleration due to gravity = 9.81 m s^{-2}) and conversion factor.

The relationships between soil attributes and between these and water retention were investigated by constructing correlation matrices in R (R Core Team 2021) using the package *corrplot* (Wei & Simko 2021). A t test was applied to each correlation coefficient at 5 % significance using the package *Hmisc* (Harrel 2021). To compare the different peatlands (Chapada and Pinheiro) and vegetation types (grassland and forest), principal component analysis was conducted on the soil attributes using the packages *FactoMineR* (Le *et al*. 2008) and *factoextra* (Kassambara & Mundt 2020).

RESULTS

Mass and volume relationships

Bulk density and organic matter content varied between depths, peatlands and vegetation (Table 1). Organic matter comprised 13.5–75.0 % of the organic layers in the sampled cores. Mineral matter content was usually higher under *capão* (woody) vegetation and in the deeper peat layers. Peatlands under *campo* (grassland) vegetation often presented higher organic matter content and lower bulk density, ranging from 0.10 to 0.77 Mg m^{-3}, whereas bulk density values under *capão* vegetation ranged from 0.19 to 1.11 Mg m^{-3}.

Bulk density was strongly affected by the mineral and organic matter contents, with correlation coefficients of 0.907 and -0.907, respectively (not shown). Bulk density values > 0.4 Mg m^{-3} were observed only in layers with more than 38 % mineral matter, and bulk density values > 0.6 Mg m^{-3} occurred only in layers with more than 63 % mineral matter.

Organic matter characterisation

The results for humic substances fractionation (fulvic and humic acids and humin fractions), rubbed and unrubbed fibre contents, cellulose and lignin contents, C:N ratio, chemical composition (C and N contents) and isotopic C content are provided in the Supplementary Material (as an Excel file). These results have been discussed by Horák-Terra *et al.* (2014) and Silva *et al.* (2019), so our main focus here is on the relationships of these properties with the water retention characteristics of the peat.

Only a few significant correlations were obtained amongst these attributes (Figure 3). The chemical fractionation of humic substances was poorly related to the other attributes and significant correlations were observed only between the different humic fractions. The rubbed and unrubbed fibre contents did not present significant correlations to any other evaluated attributes.

Table 1. Organic and mineral matter content (loss on ignition) and bulk density for the evaluated depths of the Chapada and Pinheiro peatlands under *campo* (grassland) and *capão* (forest).

Site	*campo* (grassland vegetation)				*capão* (forest vegetation)			
	Depth (cm)	Organic matter (%)	Mineral matter (%)	Bulk density (Mg m^{-3})	Depth (cm)	Organic matter (%)	Mineral matter (%)	Bulk density (Mg m^{-3})
Chapada	0–15	69.9	30.1	0.11	0–15	63.6	36.4	0.24
	15–30	48.2	51.8	0.18	15–30	66.4	33.6	0.27
	30–45	33.6	66.4	0.61	30–45	49.7	50.3	0.45
	45–60	51.1	48.9	0.24	45–60	36.6	63.4	0.60
	60–75	22.4	77.6	0.77	60–75	13.5	86.5	1.11
	75–90	20.3	79.7	0.74	75–90	21.0	79.0	0.96
	90–105	33.9	66.1	0.22	90–105	16.3	83.7	1.01
					105–120	15.1	84.9	0.93
					120–135	16.4	83.6	0.98
Pinheiro	0–15	75.0	25.0	0.10	0–15	63.3	36.7	0.19
	15–30	68.6	31.4	0.11	15–30	68.8	31.2	0.29
	30–45	62.0	38.0	0.18	30–45	67.1	32.9	0.24
	45–60	64.0	36.0	0.20	45–60	34.3	65.7	0.49
	60–75	59.2	40.8	0.23	60–75	21.3	78.7	0.77
	75–90	61.5	38.5	0.46	75–90	15.0	85.0	0.29

The soil and organic matter attributes reflected the differences between peatlands and vegetation (Figure 4). Although the first two principal components of the principal components analysis accounted for only about half of the data variability, they related well to most of the variables. The humic fractions and the rubbed/unrubbed fibre contents related more strongly to the third and fourth principal components, which accounted for 13.4 % and 9.2 % of the total variance. The first principal component reflected the influence of soil structure (bulk density) and composition (organic and mineral matter content), while the second principal component reflected the effect of vegetation, being strongly influenced by lignin content and $\delta^{13}C$.

The average points for the peatlands under forest vegetation (larger circles in Figure 4) were closely clustered together and indicated a greater similarity between these sites than between the others. The second principal component was especially important for separating the points under *capão* (higher lignin content and more negative $\delta^{13}C$ values), but these sites also tended to present higher bulk density, higher mineral matter content (Table 1) and a more advanced stage of organic matter decomposition, as indicated by the higher organic matter specific weight and higher C:N ratio (Supplementary Material).

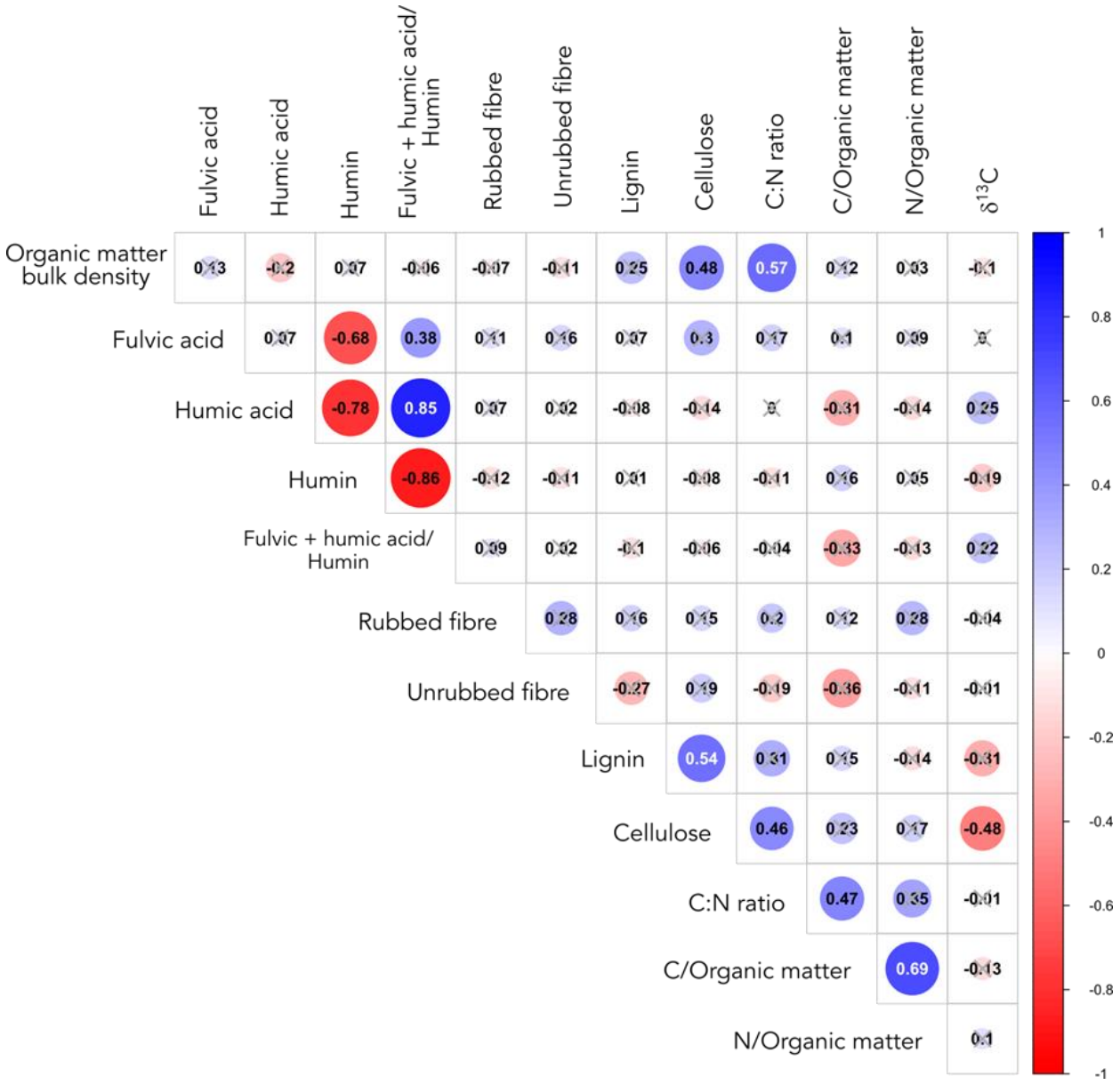

Figure 3. Correlation matrix between soil and organic matter attributes from the studied peatlands. Non-significant correlations are marked '×'.

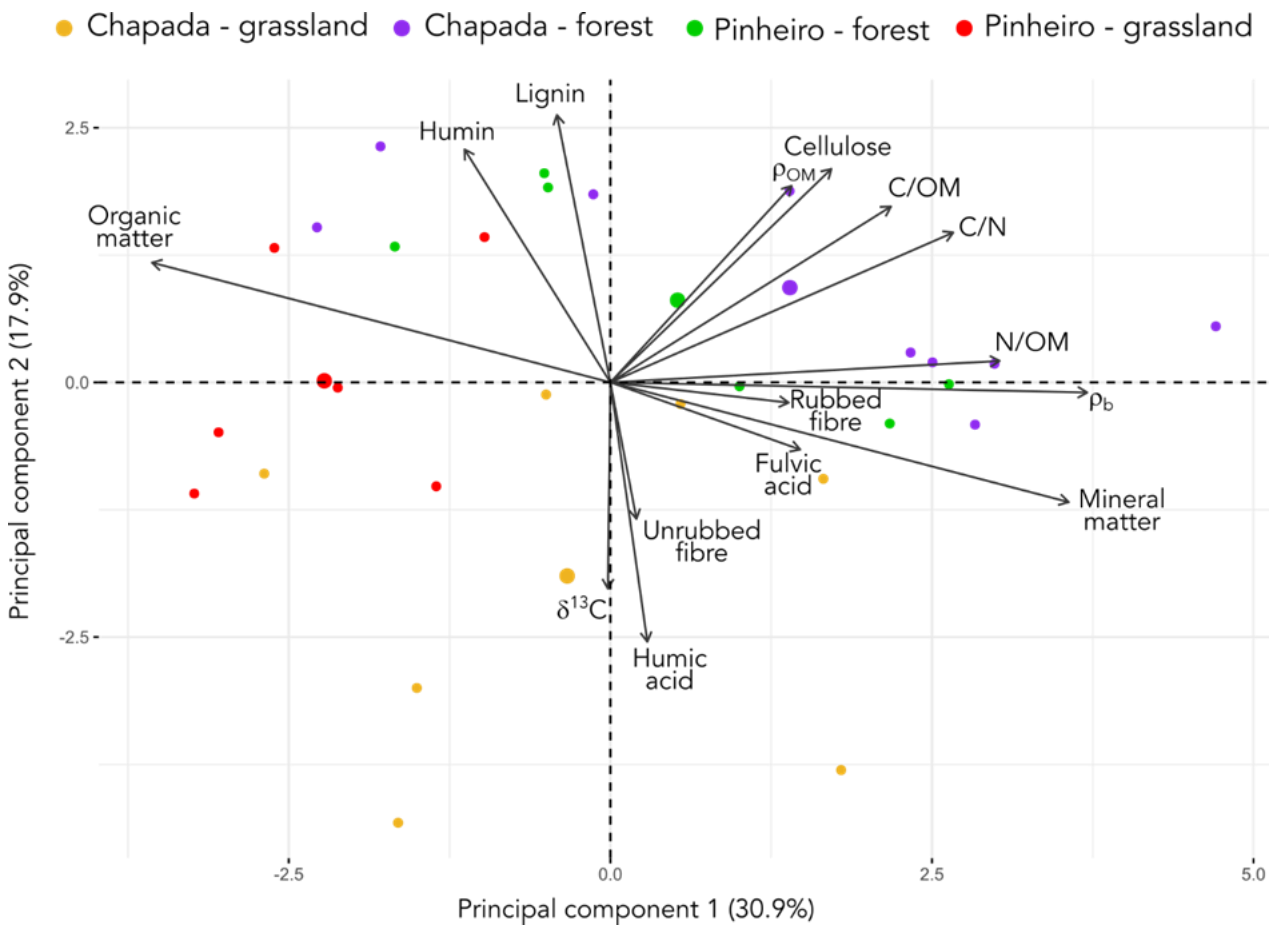

Figure 4. Biplot of the principal component analysis for soil and organic matter attributes from the studied peatlands (Pinheiro and Chapada) under grassland (*campo*) and forest (*capão*) vegetation. ρ_b = bulk density; ρ_{OM} = organic matter bulk density; C/OM = carbon content in the organic matter; N/OM = nitrogen content in the organic matter.

Water retention

Water retention was very high under higher matric potentials (less negative and closer to zero), and the water retention curves presented an initially smooth decrease in water content followed by a sharp decrease for water potentials (Ψ) beyond -7,000 cm (Figures 5 and 6). The water retention data fitted well to the bimodal curves, with RMSE values ranging from < 0.001 to 0.030 $m^3\ m^{-3}$ (Table 2).

The bimodal water retention curves (Figure 6) indicated that the pore structure of the organic soils was heterogeneous (Durner 1994) and that two distinct behaviours occurred within the evaluated range of water potentials. For water tensions up to 7,000 cm, the retention curves showed a smooth sigmoid behaviour. Beyond this, the curves descended very steeply until a new asymptote was reached close to -12,000 cm matric potential. This behaviour was reflected in the variation of the adjusted parameters for each of the subsystem curves (Table 2). For the parameter *n*, which controls the

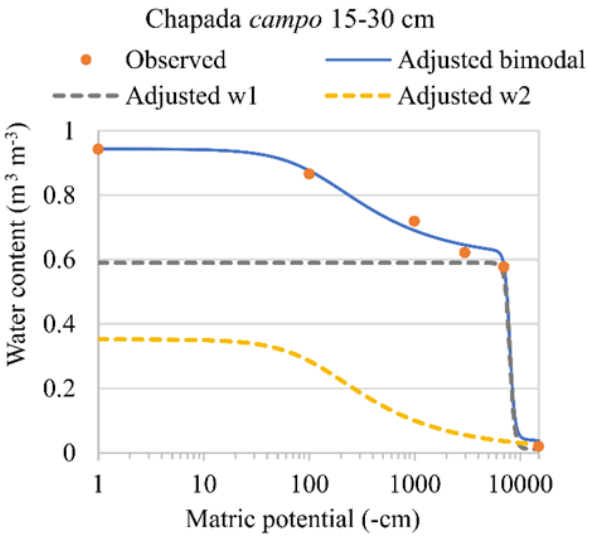

Figure 5. Example of the adjusted bimodal water retention curves based on the van Genuchten model. The bimodal retention curve (blue line) results from the sum of the two others (w1 and w2).

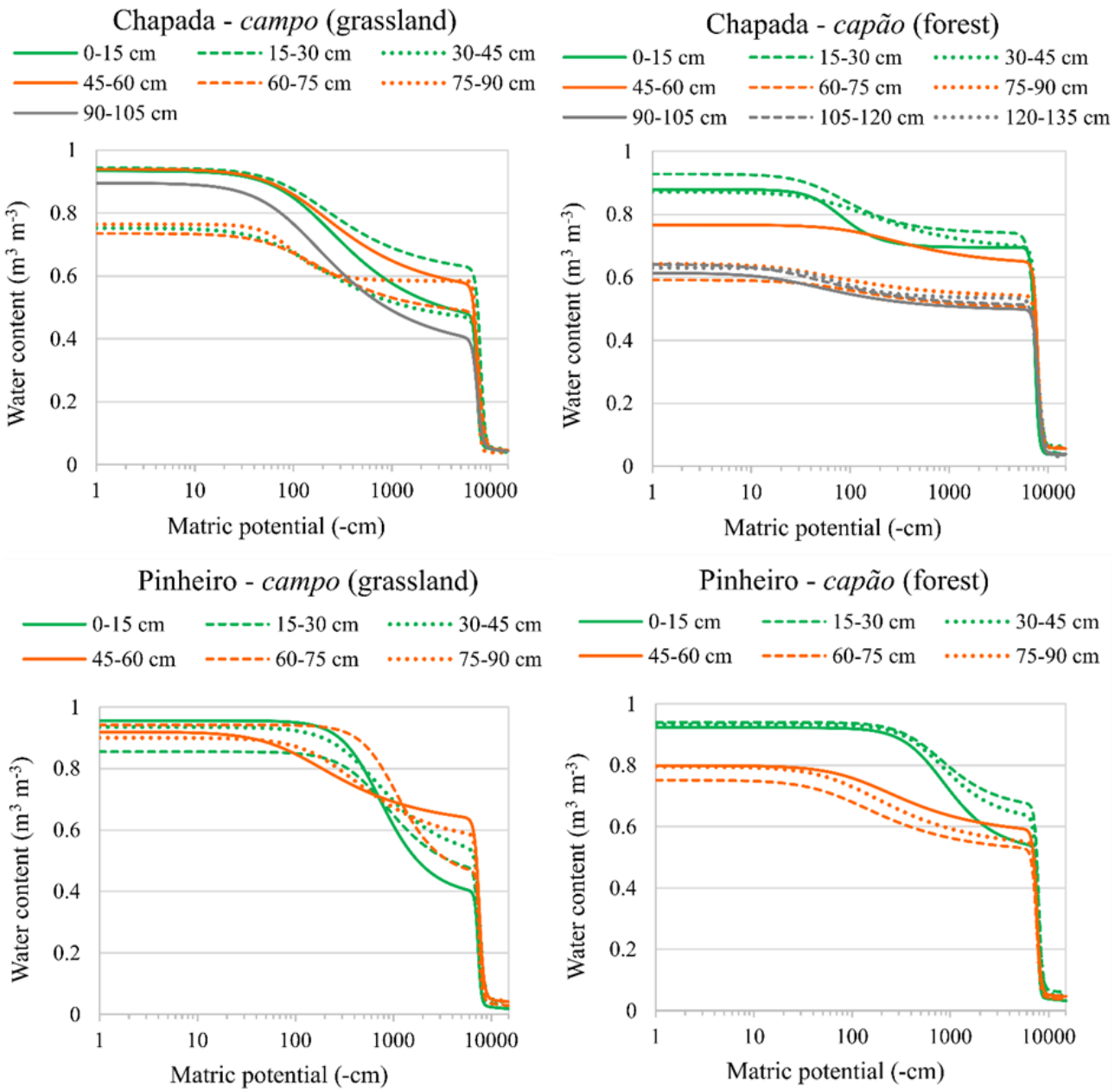

Figure 6. Bimodal water retention curves for the evaluated layers from both peatlands (Chapada and Pinheiro) under forest and grassland vegetation (*campo* and *capão*, respectively).

steepness of the curve (de Jong van Lier 2020), the smooth sigmoid parts of the curves at higher matric potentials presented much lower values (n_2=1.52–2.89) than the steeper parts of the curves corresponding to the lower matric potentials (n_1=12.6–36.7).

The individual contributions of the two subsystems that described the entire water retention behaviour of the evaluated soils were distinctive (Table 2). These were measured by the parameters w_1 and w_2, which sum to unity ($w_1 + w_2 = 1$). The parameter w_1, which described the drier part of the retention curve, ranged from 0.39 to 0.84. The higher its value, the greater the proportion of total water content that was retained in this drier subsystem of the curve; and the lower its value, the higher the w_2 value and the higher the amount of water retained in the subsystem corresponding to higher matric potentials.

Pore size distribution

Total porosity, as indicated by the water content at saturation (Table 2), varied from 59 % to 95.5 %. The discrete pore size distribution according to classes of

Table 2. Water retention at saturation (θ_s), residual water content (θ_r), fitted parameters (w_1, α_1, n_1, w_2, α_2, n_2) for the water retention curves, R^2 and RMSE values.

Site	Depth (cm)	θs (m^3 m^{-3})	θr (m^3 m^{-3})	w_1	α_1	n_1	w_2	α_2	n_2	R^2	RMSE (m^3 m^{-3})
Chapada – *campo* (grassland)	0–15	0.934	0.013	0.45	0.00014	26.4	0.55	0.0076	1.60	0.991	0.030
	15–30	0.942	0.020	0.63	0.00013	19.1	0.37	0.0085	1.61	0.997	0.017
	30–45	0.752	0.033	0.57	0.00013	18.8	0.43	0.0114	1.58	0.995	0.017
	45–60	0.939	0.022	0.56	0.00014	20.8	0.44	0.0089	1.57	0.992	0.027
	60–75	0.735	0.034	0.62	0.00013	17.1	0.38	0.0099	1.64	0.999	0.009
	75–90	0.763	0.039	0.75	0.00014	28.2	0.25	0.0120	2.89	0.999	0.001
	90–105	0.895	0.015	0.39	0.00014	18.1	0.61	0.0106	1.58	0.991	0.029
Chapada – *capão* (forest)	0–15	0.878	0.037	0.78	0.00014	22.5	0.22	0.0148	2.76	0.999	0.007
	15–30	0.929	0.040	0.79	0.00013	12.6	0.21	0.0170	2.01	0.999	<0.001
	30–45	0.872	0.051	0.76	0.00013	20.8	0.24	0.0136	1.52	0.999	0.016
	45–60	0.767	0.049	0.82	0.00013	22.3	0.18	0.0067	1.60	0.999	0.009
	60–75	0.592	0.055	0.83	0.00013	21.8	0.17	0.0180	1.54	0.999	0.005
	75–90	0.643	0.056	0.82	0.00013	22.3	0.18	0.0321	1.52	0.999	0.006
	90–105	0.615	0.035	0.79	0.00013	20.8	0.21	0.0404	1.55	0.999	0.004
	105–120	0.641	0.032	0.78	0.00013	20.7	0.22	0.0384	1.57	0.999	0.004
	120–135	0.631	0.030	0.84	0.00013	14.3	0.16	0.0202	2.09	0.999	<0.001
Pinheiro – *campo* (grassland)	0–15	0.955	0.012	0.39	0.00014	27.8	0.61	0.0018	2.33	0.999	0.006
	15–30	0.854	0.013	0.51	0.00014	27.8	0.49	0.0017	2.03	0.993	0.027
	30–45	0.935	0.019	0.52	0.00013	20.6	0.48	0.0022	1.88	0.994	0.026
	45–60	0.919	0.022	0.65	0.00013	19.0	0.35	0.0106	1.55	0.994	0.023
	60–75	0.941	0.021	0.46	0.00013	27.5	0.54	0.0011	2.49	0.997	0.022
	75–90	0.900	0.025	0.60	0.00013	29.6	0.40	0.0042	1.71	0.997	0.016
Pinheiro – *capão* (forest)	0–15	0.922	0.025	0.55	0.00013	36.7	0.45	0.0016	2.22	0.999	0.013
	15–30	0.939	0.053	0.68	0.00013	22.8	0.32	0.0017	2.12	0.999	0.010
	30–45	0.933	0.040	0.64	0.00013	21.4	0.36	0.0016	2.17	0.999	0.011
	45–60	0.798	0.033	0.70	0.00013	21.3	0.30	0.0079	1.60	0.997	0.014
	60–75	0.752	0.026	0.67	0.00013	19.8	0.33	0.0135	1.59	0.998	0.010
	75–90	0.796	0.025	0.65	0.00013	28.0	0.35	0.0109	1.58	0.997	0.015

pore diameter indicated a vast predominance of micropores (Figure 7), with equivalent pore diameter in the range 0.2–3 µm (matric potentials of -15,000 and -1,000 cm, respectively), ranging from 0.34 to 0.75 m^3 m^{-3}. These pores are related to the retention of plant available water, and are likely to allow for adequate water availability for the vegetation throughout the year, retaining from 590.8 to 777 mm of water in the evaluated peat cores. The volume of macropores was unexpectedly low for such porous soils, with an overall average of 0.07 m^3 m^{-3}. These pores, along with the mesopores (ranging from 0.03 to 0.32 m^3 m^{-3}), would be more important for sustaining water flow throughout the year. Macropores and mesopores combined could provide 150–256 mm of water considering the depth of the

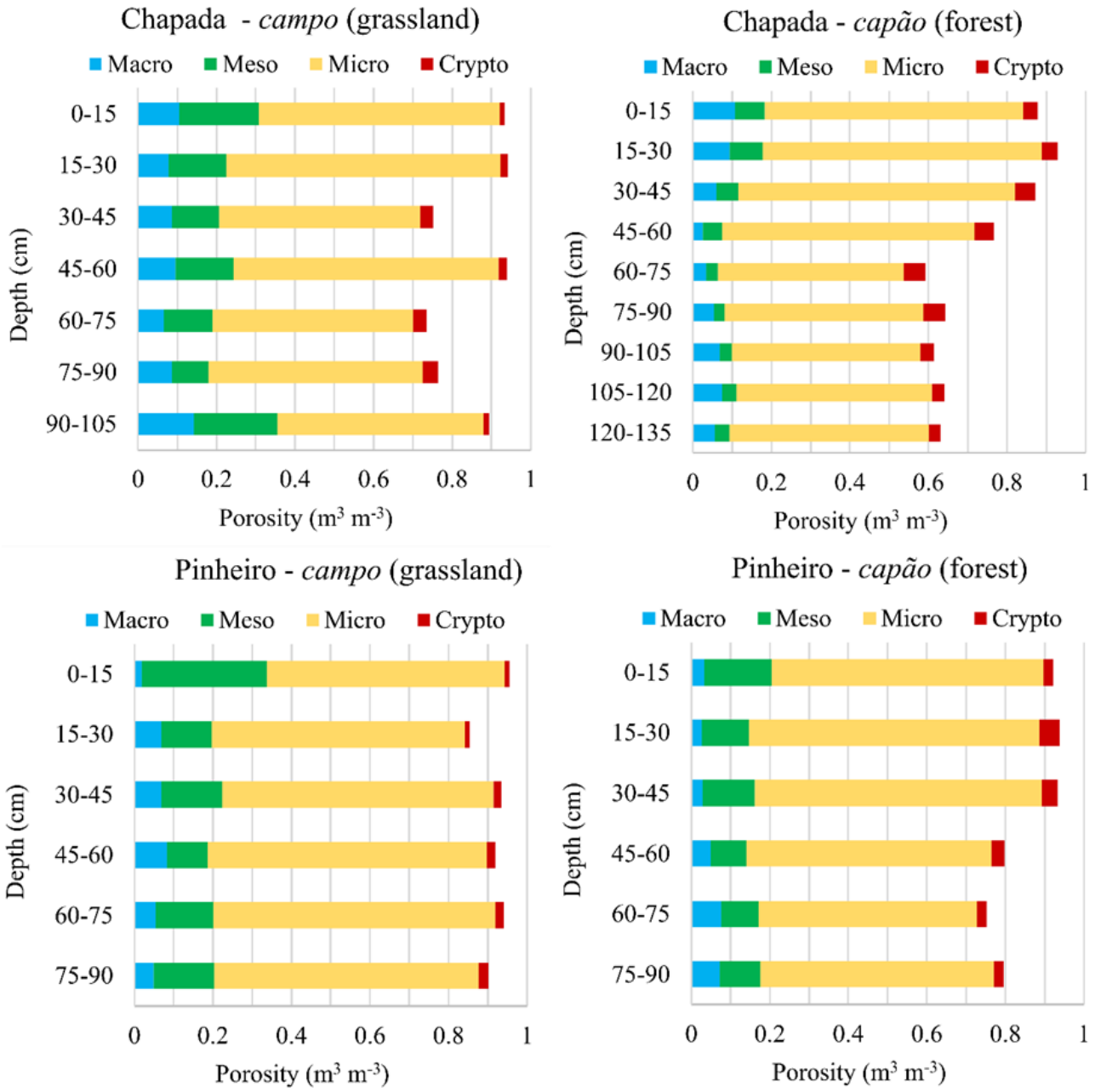

Figure 7. Discrete pore size distribution in the classes macropores, mesopores, micropores and cryptopores for the evaluated layers from both peatlands (Chapada and Pinheiro) under forest (*campo*) and grassland (*capão*) vegetation.

sampled cores. The cryptopores (pore diameter < 0.2 µm, retained water unavailable to plants) were least abundant, occupying only 0.01–0.05 m^3 m^{-3}, because of the low bulk density and the predominance of sand in the mineral matter.

The bimodal water retention curves fitted to the data resulted in pore size distributions showing two distinct peaks (Figure 8). Each peak in the continuous pore size distribution corresponds to a modal diameter (the most common equivalent pore diameter) and these peaks occur at the inflection points of the water retention curves. The deeper layers commonly peaked at larger pore diameters, even though these layers presented higher bulk density and higher mineral matter content than shallower layers (Table 1).

The peaks relating to the smaller pores occurred within a narrow range of diameters, from 0.38 to 0.41 µm. Although they may be perceived as causing just a small peak in the pore size distribution curves, these pores accounted for 39–84 % of the water retained between saturation and the permanent

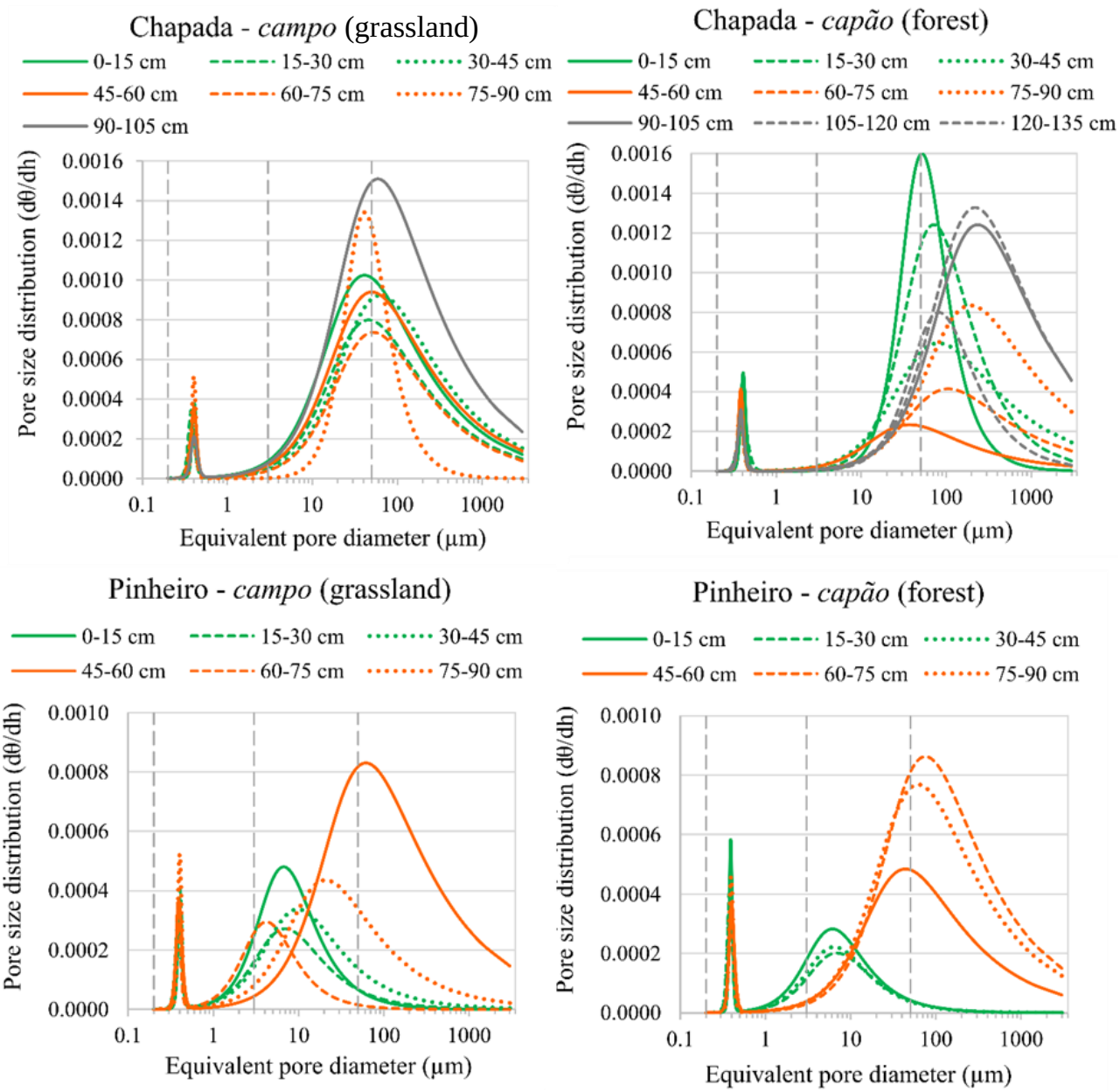

Figure 8. Continuous pore size distributions as given by the first derivative of the bimodal water retention curves for the evaluated layers from both peatlands (Chapada and Pinheiro) under forest (*campo*) and grassland (*capão*) vegetation. Vertical dashed lines indicate the limits between pore size classes (macropores > 50 µm; mesopores 3–50 µm; micropores 0.2–3 µm and cryptopores < 0.2 µm).

wilting point, as indicated by the w_1 values in Table 2. The peak relating to the larger pores varied much more broadly, ranging from 4.2 to 229 µm.

Relating water retention to soil attributes

As can be seen from the correlation matrix in Figure 9, water retention and pore size distributions in these peatland soils was significantly related to soil structure (bulk density), composition (mineral and organic matter content) and organic matter properties, which in turn were affected by degree of decomposition (organic matter specific weight, C:N ratio) and vegetation (lignin and cellulose contents). Chemical fractionation of humic substances (fulvic and humic acids and humin fractions) and physical fractionation of fibres (rubbed and unrubbed fibre contents) often presented weak and non-significant relationships with water retention and pore size distribution.

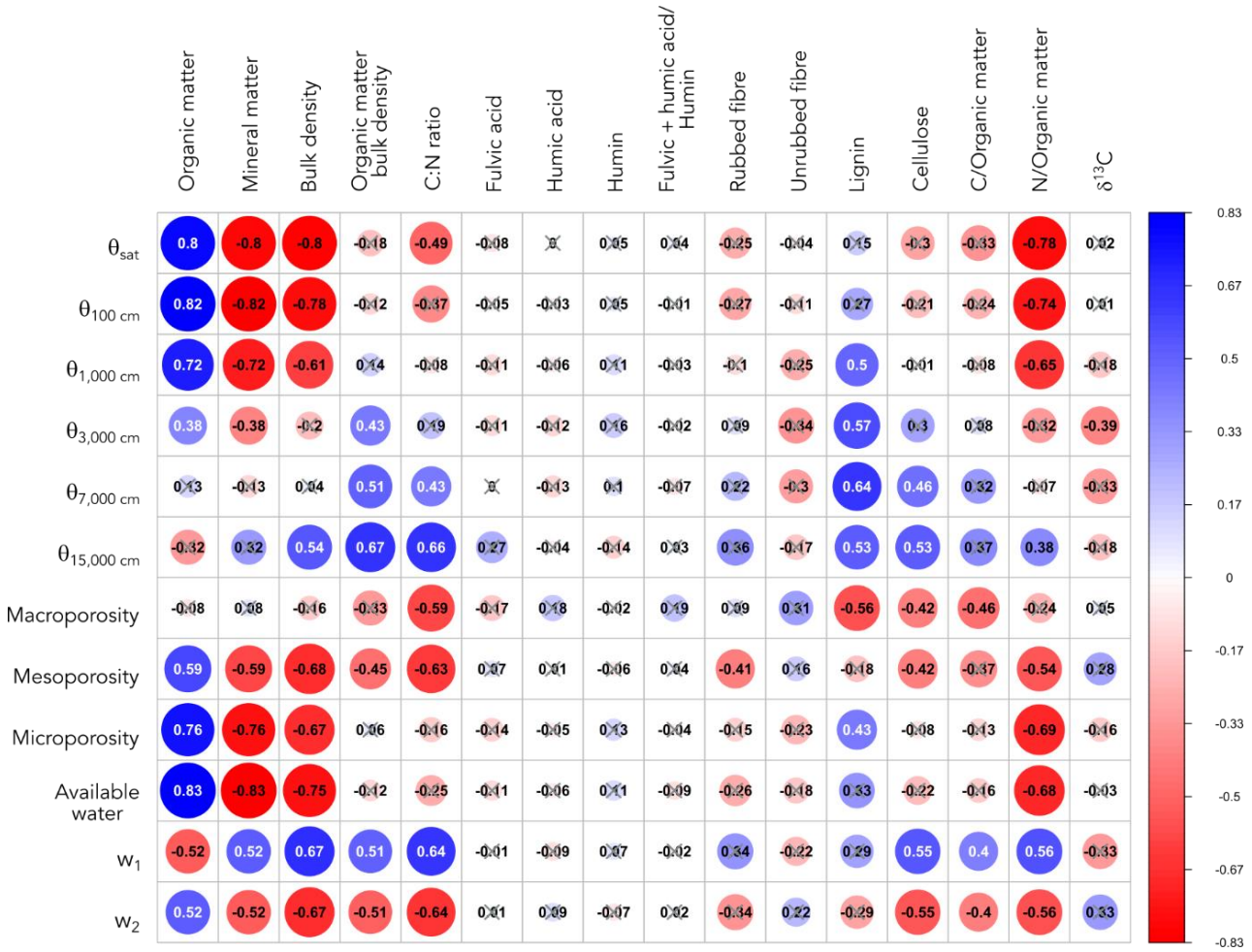

Figure 9. Correlation matrix between water retention and pore size distribution and the soil and organic matter attributes from the studied peatlands. Non-significant correlations are marked '×'.

Macroporosity in general did not correlate well to the variables that more strongly affected the water content at higher (less negative) matric potentials. It was significantly related only to degree of decomposition and lignocellulosic composition (C:N ratio, lignin and cellulose content, C content in the organic matter), with negative correlations. On the other hand, mesoporosity, microporosity and available water capacity presented the same overall trends as water retention, with higher values related to lower bulk density and higher organic matter content.

DISCUSSION

Soil attributes

On peatlands from the Espinhaço Range with 9.7–40.2 % of organic carbon (the range was 7.6–36 % in the present study), Bispo *et al.* (2016) obtained similar bulk density values to those reported here, ranging from 0.09 to 1.09 Mg m^{-3} under grassland vegetation and from 0.14 to 0.55 Mg m^{-3} under forest vegetation. Our bulk density values are also similar to those observed by Horák-Terra *et al.* (2014) in histic horizons from several peatlands of this same region, which ranged from 0.08 to 1.14 Mg m^{-3}.

Although organic matter decomposition and compression of basal layers are important factors affecting bulk density in peatlands (Gnatowski *et al.* 2010), Horák-Terra *et al.* (2014) also observed that mineral matter content was a major factor affecting bulk density in peatlands from the Espinhaço Range. According to Campos *et al.* (2017), the occurrence of sand layers is common in these peatlands because they often occupy flat valley bottoms that receive water and sediment flows from the shallow soils upslope. Erosion processes play an important role in the evolution of these Histosols, especially under drier climate (Horák-Terra *et al.* 2014), which affects their physical and hydraulic properties.

The first principal component in Figure 4 highlighted the difference between peatlands, with

the Pinheiro peatland presenting more organic matter and lower bulk density than the Chapada peatland. According to Campos *et al.* (2017), the Chapada peatland is a hanging bog, while the Pinheiro peatland is classified as a structural bog. A hanging bog was defined by the authors as a peatland occurring at the bottom of a valley in quartzite terrain, like the concept of valley fen from Lindsay (2018). A structural bog was defined as peatland that formed because of rock strata that hampered water drainage and could be interpreted as a percolation fen in the Lindsay (2018) classification. Given this classification, the higher bulk density and mineral matter content in the Chapada peatland could be related to its position at the valley bottom, where it would receive more sandy sediments from upslope areas than would the Pinheiro peatland.

Rubbed and unrubbed fibre content and the chemical fractionation of humic substances resulted in poor correlations with other soil and organic matter attributes (Figures 3 and 9). The analysis of rubbed and unrubbed fibre content proposed by Lynn *et al.* (1974) has been adopted as an official technique for the characterisation of organic soils in Brazil (Santos *et al.* 2018). Rubbed and unrubbed fibre contents required laborious determination and yet failed to reflect the other attributes evaluated in the present study. Although the fractionation of humic substances may correlate well to some properties of soil organic matter such as degree of decomposition and cation exchange capacity (Hayes & Swift 2020), alkali extraction of humic substances can be misleading with regard to the wide range of decomposed and undecomposed molecules retained at each fraction (Kleber & Lehmann 2019).

On the other hand, cellulose and lignin contents presented significant correlations with attributes that reflect the degree of decomposition of organic matter and the influence of different vegetation types. Cellulose content was the only attribute significantly related to $\delta^{13}C$ (correlation coefficient of -0.48), indicating that it can reflect the influence of vegetation on soil organic matter. Cellulose content also presented significant correlations with organic matter specific weight and C:N ratio, which may reflect the degree of decomposition of soil organic matter (Horák-Terra *et al.* 2014).

Water retention

The observed water retention behaviour was captured by fitting bimodal water retention curves, which were the only equations capable of properly describing it. The overall forms of the curves can be regarded as a juxtaposition of two van Genuchten models (van Genuchten 1980), and this is precisely what the bimodal water retention curve does, by treating the water retention curve as the sum of two van Genuchten equations (Durner 1994, de Jong van Lier 2020). According to Durner (1994), multimodal water retention curves are especially important for modelling hydraulic conductivity near saturation. Our results indicated that the bimodal retention curve was important for modelling the pore size distribution towards the drier portion of the curve, especially for water potentials lower than -7,000 cm. In this sense, the use of conventional unimodal retention curves could be appropriate for modelling the hydraulic conductivity of peatland soils from a hydrological perspective, as the fitted curve would depart strongly from the observed data only towards the drier portion of the curve. However, when the retention curve is to be used for evaluating plant available water, the multimodal pore size distributions ought to be better descriptors of the water retention behaviour of peatland soils. This may be especially relevant for peatlands (such as those in the present study) that have been affected by the erosional deposition of mineral particles, which promotes multimodal (particularly bimodal) pore size distributions.

It is possible that this bimodal behaviour of the water retention curve and pore size distribution have been overlooked in previous studies because of the methodological procedures sometimes adopted, with a large gap between applied pressures towards the permanent wilting point. For example, John *et al.* (2021) applied 500 cm before 15,000 cm, while Kurnain (2019) applied 1,000 cm, usually resulting in smooth curves between these pressures and the last point at 15,000 cm. Nevertheless, Dettmann *et al.* (2014) also observed that bimodal water retention curves provided a better description of the hydraulic conductivity of peatland soils at different decomposition stages, because the bimodal model better captured the behaviour of macropore flow. Weber *et al.* (2017) observed a trimodal pore-size distribution in living and decomposed *Sphagnum*, within the range of matric potentials from -10,000 cm to saturation, considering this to reflect the different porous spaces within and between plant tissues.

The tremendous water holding capacity of these tropical mountain peatlands has already been acknowledged in previous studies (Campos *et al.* 2011, Silva *et al.* 2013a), and the present study further investigated the water retention behaviour of these organic soils. Despite their enormous water content at saturation (Table 2), the amount of water available to sustain river flow is only a fraction of this. The water retention curves (Figure 6) indicate that water content remains substantially high at

matric potentials down to -1,000 cm and this comprises the more loosely bound water. Although much water is still retained beyond this matric potential, its importance in sustaining water flow remains to be determined, as we did not evaluate saturated and unsaturated hydraulic conductivity. Given the bimodal nature of the porous system, we might expect a relatively smooth decrease in hydraulic conductivity along the smooth sigmoid portion of the retention curve, with a steep decline as the soil dries further. Therefore, to understand the hydrological behaviour of these soils it is imperative to assess their hydraulic conductivity.

Relating water retention to soil attributes

Water retention at higher potentials, from -1,000 cm to saturation, was more strongly affected by soil structure, with significant correlations to bulk density and mineral/organic matter content. These factors became less and less important for water retention at lower matric potentials, while degree of decomposition and lignocellulosic content of the organic matter became increasingly more important. For water retention at -15,000 cm, bulk density was also significant, but with a positive correlation coefficient. It was also observed by John *et al.* (2021) that bulk density was a better predictor for water retention at saturation and at the permanent wilting point, whereas fibre content was a better predictor at the intermediate matric potentials.

The bimodal water retention curves were also significantly affected by soil attributes, as indicated by the correlations with the parameters w_1 and w_2. These parameters are related to the water retention at lower water potentials (w_1) and higher water potentials (w_2), respectively. The parameter w_1 was positively related to bulk density, mineral matter content and degree of decomposition (organic matter specific weight and C:N ratio), reflecting higher water retention at lower water potentials in denser soil. The parameter w_2 behaved inversely (as $w_1 + w_2 = 1$), indicating a greater contribution of this subsystem at higher organic matter contents.

ACKNOWLEDGEMENTS

Support for the current study was provided by the Brazilian National Council on Scientific and Technological Development (CNPq), the Coordenação de Aperfeiçoamento de Pessoal de Nível Superior (CAPES) of Brazil, and the state Fundação de Amparo à Pesquisa de Minas Gerais (FAPEMIG).

AUTHOR CONTRIBUTIONS

PGSS and ACS designed the study and were aided in the fieldwork by CRC, UMB and IH-T. PGSS conducted the laboratory analysis. WJC was essential to the revision process. DT performed the statistical analysis and drafted the manuscript, which was carefully reviewed, improved, and approved by the other authors.

REFERENCES

Bechtold, M., Dettmann, U., Wöhl, L., Durner, W., Piayda, A., Tiemeyer, B. (2018) Comparing methods for measuring water retention of peat near permanent wilting point. *Soil Science Society of America Journal*, 82(3), 601–605. https://doi.org/10.2136/sssaj2017.10.0372

Benites, V.M., Machado, P.L.O.A., Madari, B.E., Fontana, A. (2017) Fracionamento químico da matéria orgânica (Organic matter chemical fractionation). In: Teixeira, P.C., Donagemma, G.K., Fontana, A., Teixeira, W.G. (eds.) *Manual de Métodos de Análise de Solo* (*Manual of Soil Analysis Methods*), Embrapa, Brasília DF, 401–414 (in Portuguese).

Bispo, D.F.A., Silva, A.C., Christofaro, C., Silva, M.L.N., Barbosa, M.S., Silva, B.P.C., Barral, U.M., Fabris, J.D. (2016). Hydrology and carbon dynamics of tropical peatlands from Southeast Brazil. *Catena*, 143, 18–25. https://doi.org/10.1016/j.catena.2016.03.040

Campos, J.R.R., Silva, A.C., Fernandes, J.S.C., Ferreira, M.M., Silva, D.V. (2011) Water retention in a peatland with organic matter in different decomposition stages. *Revista Brasileira de Ciência do Solo*, 35(4), 1217–1227. https://doi.org/10.1590/S0100-06832011000400015

Campos, J.R.R., Silva, A.C., Vidal-Torrado, P. (2012) Mapping, organic matter mass and water volume of a peatland in Serra do Espinhaço Meridional. *Revista Brasileira de Ciência Do Solo*, 36(3), 723–732. https://doi.org/10.1590/S0100-06832012000300004

Campos, J.R.R., Silva, A.C., Nanni, M.R., Santos, M., Vidal-Torrado, P. (2017) Influence of the structural framework on peat bog distribution in the tropical highlands of Minas Gerais, Brazil. *Catena*, 156, 228–236. https://doi.org/10.1016/j.catena.2017.04.018

de Jong van Lier, Q. (2020) *Física do Solo baseada em processos (Process-based Soil Physics).* CENA/USP, Piracicaba SP, 413 pp. Online at: http://www.cena.usp.br/publicacao/fisica_solo_b

aseada_processos.pdf (in Portuguese).

Dettmann, U., Bechtold, M. (2016) Deriving effective soil water retention characteristics from shallow water table fluctuations in peatlands. *Vadose Zone Journal*, 15(10), 1–13. https://doi.org/10.2136/vzj2016.04.0029

Dettmann, U., Bechtold, M., Frahm, E., Tiemeyer, B. (2014) On the applicability of unimodal and bimodal van Genuchten-Mualem based models to peat and other organic soils under evaporation conditions. *Journal of Hydrology*, 515, 103–115. https://doi.org/10.1016/j.jhydrol.2014.04.047.

Dimitrov, D.D., Lafleur, P.M. (2021) Revisiting water retention curves for simple hydrological modelling of peat. *Hydrological Sciences Journal*, 66(2), 252–267. https://doi.org/10.1080/02626667.2020.1853132

Durner, W. (1994) Hydraulic conductivity estimation for soils with heterogeneous pore structure. *Water Resources Research*, 30, 211–223.

Finlayson, C.M., Milton, G.R. (2018) Peatlands. In: Finlayson, C.M., Milton, G.R., Prentice, R.C., Davidson, N.C. (eds.) *The Wetland Book*, Springer, Dordrecht, 227–244.

Fontana, A. (2017) Matéria orgânica (Organic matter). In: Teixeira, P.C., Donagemma, G.K., Fontana, A., Teixeira, W.G. (eds.) *Manual de Métodos de Análise de Solo* (*Manual of Soil Analysis Methods*), Embrapa, Brasília DF, 397–400 (in Portuguese).

Fontana, A.; Bianchi, S.R. (2017) Carbono e nitrogênio total - analisador elementar (Total carbon and nitrogen - elemental analyser). In: Teixeira, P.C., Donagemma, G.K., Fontana, A., Teixeira, W.G. (eds.) *Manual de Métodos de Análise de Solo* (*Manual of Soil Analysis Methods*), Embrapa, Brasília DF, 393–396 (in Portuguese).

Gnatowski, T., Szatyłowicz, J., Brandyk, T., Kechavarzi, C. (2010) Hydraulic properties of fen peat soils in Poland. *Geoderma*, 154(3–4), 188–195. https://doi.org/10.1016/j.geoderma.2009.02.021

Hayes, M.H.B., Swift, R.S. (2020) Vindication of humic substances as a key component of organic matter in soil and water. *Advances in Agronomy*, 163, 1–37. https://doi.org/10.1016/bs.agron.2020.05.001

Harrell, F.E.Jr. (2021) *Hmisc: Harrell Miscellaneous*. Version 4.6-0. Online at: https://CRAN.R-project.org/package=Hmisc, accessed 03 Feb 2022.

Horák-Terra, I., Cortizas, A.M., Camargo, P.B., Silva, A.C., Vidal-Torrado, P. (2014) Characterization of properties and main processes related to the genesis and evolution of tropical mountain mires from Serra do Espinhaço Meridional, Minas Gerais, Brazil. *Geoderma*, 232–234, 183–197. https://doi.org/10.1016/j.geoderma.2014.05.008

Horák-Terra, I., Cortizas, A.M., Luz, C.F.P., López, P.R., Silva, A.C., Vidal-Torrado, P. (2015) Holocene climate change in central-eastern Brazil reconstructed using pollen and geochemical records of Pau de Fruta mire (Serra do Espinhaço Meridional, Minas Gerais). *Palaeogeography, Palaeoclimatology, Palaeoecology*, 437, 117–131. https://doi.org/10.1016/j.palaeo.2015.07.027

Horák-Terra, I., Cortizas, A.M., Luz, C.F.P., Silva, A.C., Mighall, T., Camargo, P.B., Mendonça-Filho, C.V., Oliveira, P.E., Cruz, F.W., Vidal-Torrado, P. (2020) Late Quaternary vegetation and climate dynamics in central-eastern Brazil: insights from a ~35k cal a bp peat record in the Cerrado biome. *Journal of Quaternary Science*, 35(5), 664–676. https://doi.org/10.1002/jqs.3209

INMET (2022) *Normais climatológicas 1991–2020* (*Climate Normals 1991–2020*). Instituto Nacional de Meteorologia (INMET), Brasília DF. Online at: https://portal.inmet.gov.br/normais, accessed 03 May 2022 (in Portuguese).

John, A., Fuentes, H.R., George, F. (2021) Characterization of the water retention curves of Everglades wetland soils. *Geoderma*, 381, 114724, 14 pp. https://doi.org/10.1016/j.geoderma.2020.114724

Kassambara, A., Mundt, F. (2020) *factoextra: Extract and Visualize the Results of Multivariate Data Analyses*. Version 1.0.7. Online at: https://CRAN.R-project.org/package=factoextra, accessed 03 Feb 2022

Kelly, T.J., Lawson, I.T., Roucoux, K.H., Baker, T.R., Coronado, E.N.H. (2020) Patterns and drivers of development in a west Amazonian peatland during the late Holocene. *Quaternary Science Reviews*, 230, 106168, 18 pp. https://doi.org/10.1016/j.quascirev.2020.106168

Kleber, M., Lehmann, J. (2019) Humic substances extracted by alkali are invalid proxies for the dynamics and functions of organic matter in terrestrial and aquatic ecosystems. *Journal of Environmental Quality*, 48(2), 207–216. https://doi.org/10.2134/jeq2019.01.0036

Kock, S.T., Schittek, K., Wissel, H., Vos, H., Ohlendorf, C., Schäbitz, F., Lupo, L.C., Kulemeyer, J.J., Lücke, A. (2019) Stable oxygen isotope records ($\delta^{18}O$) of a high-Andean cushion peatland in NW Argentina (24° S) imply South American summer monsoon related moisture changes during the late Holocene. *Frontiers in Earth Science*, 7(45), 1–18. https://doi.org/

10.3389/feart.2019.00045

Kurnain, A. (2019) Hydrophysical properties of ombrotrophic peat under drained peatlands. *International Agrophysics*, 33(3), 277–283. https://doi.org/10.31545/intagr/110773

Le, S., Josse, J., Husson, F. (2008) FactoMineR: An R package for multivariate analysis. *Journal of Statistical Softwar*e, 25(1), 1–18. https://doi.org/10.18637/jss.v025.i01.

Leng, L.Y., Ahmed, O.H., Jalloh, M.B. (2019) Brief review on climate change and tropical peatlands. *Geoscience Frontiers*, 10(2), 373–380. https://doi.org/10.1016/j.gsf.2017.12.018

Lindsay, R. (2018) Peatland (mire types): Based on origin and behavior of water, peat genesis, landscape position, and climate. In: Finlayson, C.M., Milton, G.R., Prentice, R.C., Davidson, N.C. (eds.). *The Wetland Book*. Springer, Dordrecht, 251–273.

Liu, H., Lennartz, B. (2019) Hydraulic properties of peat soils along a bulk density gradient—A meta study. *Hydrological Processes*, 33(1), 101–114. https://doi.org/10.1002/hyp.13314

Lynn, W.C., McKinze, W.E., Grossman, R.B. (1974) Field laboratory tests for characterization of Histosols. In: Aandahl, A.R. (ed.) *Histosols: Their Characteristics, Classification, and Use*. Soil Science Society of America, Madison WI, 21–31. https://doi.org/10.2136/sssaspecpub6.c2

Martin, L., Flexor, J.M., Suguio, K. (1995) Vibrotestemunhador leve: Construção, utilização e possibilidades (Light vibricorer: construction, use and possibilities). *Revista do Instituto Geológico*, 16(1–2), 59–66 (in Portuguese). http://dx.doi.org/10.5935/0100-929X.19950004

Mualem, Y. (1976) A new model for predicting the hydraulic conductivity of unsaturated porous media. *Water Resources Research*, 12, 513–522. https://doi.org/10.1029/WR012i003p00513

R Core Team (2021) R: A language and environment for statistical computing. R Foundation for Statistical Computing, Vienna. Online at: https://www.R-project.org/, accessed 03 Feb 2022.

Santos, H.G., Jacomine, P.K.T., dos Anjos, L.H.C., Oliveira, V.A., Lumbreras, J.F., Coelho, M.R., Almeida, J.A., Araújo Filho, J.C., Oliveira, J.B., Cunha, T.J.F. (2018) *Sistema Brasileiro de Classificação de Solos* (*Brazilian Soil Classification System*). Embrapa, Brasília, 320–324 (in Portuguese).

Silva, A.C. (2005) Solos (Soils). In: Silva, A.C., Pedreira, L.C.V.S.F., Abreu, P.A.A. (eds.) *Serra do Espinhaço Meridional: Paisagens e Ambientes* (*Southern Espinhaço Range: Landscapes and Environments*), O Lutador, Belo Horizonte, 50–78 (in Portuguese).

Silva, M.L., Silva, A.C., Silva, B.P.C., Barral, U.M., Soares, P.G.S., Vidal-Torrado, P. (2013a) Surface mapping, organic matter and water stocks in peatlands of the Serra do Espinhaço meridional - Brazil. *Revista Brasileira de Ciência do Solo*, 37(5), 1149–1157. https://doi.org/10.1590/S0100-06832013000500004

Silva, V.E., Silva, A.C., Pereira, R.C., Camargo, P.B., Silva, B.P.C., Barral, U.M., Mendonça Filho, C.V. (2013b) Composição lignocelulósica e isótopica da vegetação e da matéria orgânica do solo de uma turfeira tropical: I - composição florística, fitomassa e acúmulo de carbono (Lignocellulosic and isotopic composition of vegetation and soil organic matter of a tropical peat: I floristic composition, biomass and carbon stock). *Revista Brasileira de Ciência do Solo*, 37(1), 121–133 (in Portuguese). https://doi.org/10.1590/S0100-06832013000100013

Silva, A.C., Barbosa, M.S., Barral, U.M., Silva, B.P.C., Fernandes, J.S.C., Viana, A.J.S., Mendonça Filho, C.V., Bispo, D.F.A., Christófaro, C., Ragonezi, C., Guilherme, L.R.G. (2019) Organic matter composition and paleoclimatic changes in tropical mountain peatlands currently under grasslands and forest clusters. *Catena*, 180, 69–82. https://doi.org/10.1016/j.catena.2019.04.017

Silva, A.C., Horàk-Terra, I., Barral, U.M., Costa, C.R., Gonçalves, S.T., Pinto, T., Christófaro Silva, B.P., Fernandes, J.S.C., Mendonça Filho, C.V., Vidal-Torrado, P. (2020) Altitude, vegetation, paleoclimate, and radiocarbon age of the basal layer of peatlands of the Serra do Espinhaço Meridional, Brazil. *Journal of South American Earth Sciences*, 103, 102728, 9 pp. https://doi.org/10.1016/j.jsames.2020.102728

Takada, M., Shimada, S., Takahashi, H. (2016*)* Tropical peat formation. In: Osaki, M., Tsuji, N. (eds.) *Tropical Peatland Ecosystems*, Springer, Tokyo, Japan, 127–135.

Taufik, M., Veldhuizen, A.A., Wösten, J.H.M., van Lanen, H.A.J. (2019) Exploration of the importance of physical properties of Indonesian peatlands to assess critical groundwater table depths, associated drought and fire hazard. *Geoderma*, 347, 160–169. https://doi.org/10.1016/j.geoderma.2019.04.001

Teixeira, W.G., Bhering, S.B. (2017) Retenção de água no solo pelos métodos da mesa de tensão e da câmara de Richards (Soil water retention by tension table and Richards chamber methods). In: Teixeira, P.C., Donagemma, G.K., Fontana, A., Teixeira, W.G. (eds.) *Manual de Métodos de*

Análise de Solo (*Manual of Soil Analysis Methods*), Embrapa, Brasília DF, 33–46 (in Portuguese).

Teixeira, P.C., Donagemma, G.K., Fontana, A., Teixeira, W.G. (eds.) (2017) *Manual de Métodos de Análise de Solo* (*Manual of Soil Analysis Methods*), third edition, Embrapa, Brasília DF (in Portuguese).

Treat, C.C., Kleinen, T., Broothaerts, N., Dalton, A.S. and 29 others (2019) Widespread global peatland establishment and persistence over the last 130,000 y. *Proceedings of the National Academy of Sciences of the United States of America*, 116(11), 4822–4827. https://doi.org/10.1073/pnas.1813305116

van Bellen, S., Mauquoy, D., Hughes, P.D.M., Roland, T.P., Daley, T.J., Loader, N.J., Street-Perrott, F.A., Rice, E.M., Pancotto, V.A., Payne, R.J. (2016) Late-Holocene climate dynamics recorded in the peat bogs of Tierra del Fuego, South America. *The Holocene*, 26(3), 489–501. https://doi.org/10.1177/0959683615609756

van Genuchten, M.T. (1980) A closed-form equation for predicting the hydraulic conductivity of unsaturated soils. *Soil Science Society of America Journal*, 44, 892–898. https://doi.org/10.2136/sssaj1980.03615995004400050002x

van Soest, P.J. (1994) *Nutritional Ecology of the Ruminant*. Cornell University Press, New York, 528 pp.

Weber, T.K.D., Iden, S.C., Durner, W. (2017) Unsaturated hydraulic properties of *Sphagnum* moss and peat reveal trimodal pore-size distributions. *Water Resources Research*, 53(1), 415–434. https://doi.org/10.1002/2016WR019707

Wei, T., Simko, V.R. (2021) *package 'corrplot': Visualization of a Correlation Matrix*. Version 0.90. Online at: https://github.com/taiyun/corrplot, accessed 03 Feb 2022.

Yu, Z., Loisel, J., Brosseau, D.P., Beilman, D.W., Hunt, S.J. (2010) Global peatland dynamics since the Last Glacial Maximum. *Geophysical Research Letters*, 37(13), L13402, 5 pp. https://doi.org/10.1029/2010GL043584

Submitted 03 Feb 2022, revision 29 Apr 2022
Editor: Olivia Bragg

Author for correspondence:
Dr Diego Tassinari, Programa de Pós-Graduação em Produção Vegetal, Universidade Federal dos Vales do Jequitinhonha e Mucuri, Rodovia MGT367 5000, 39100-000, Diamantina-MG, Brazil.
Tel: + 55 35 99941 5575; E-mail: diego.tassinari@ufvjm.edu.br

Supplementary material (available for separate download):
Excel file containing characterisation data for peat under forest (*campo*) and grassland (*capão*) vegetation at the Chapada and Pinheiro peatlands.